IET Generation, Transmission & Distribution

Research Article

IET Journals
The Institution of Engineering and Technology

New phase-changing soft open point and impacts on optimising unbalanced power distribution networks

ISSN 1751-8687
Received on 4th November 2019
Revised 7th August 2020
Accepted on 1st September 2020
E-First on 23rd October 2020
doi: 10.1049/iet-gtd.2019.1660
www.ietdl.org

Chengwei Lou[1], Jin Yang[1] ✉, Tianrui Li[2], Eduardo Vega-Fuentes[1]

[1]*James Watt School of Engineering, University of Glasgow, G12 8QQ Glasgow, UK*

[2]*State Grid Taizhou Power Supply Bureau, 318000 Zhejiang Province, People's Republic of China*

✉ *E-mail: Jin.Yang@glasgow.ac.uk*

Abstract: Three-phase unbalanced conditions in distribution networks are conventionally caused by load imbalance, asymmetrical fault conditions of transformers and impedances of three phases. The uneven integration of single-phase distributed generation (DG) worsens the imbalance situation. These unbalanced conditions result in financial losses, inefficient utilisation of assets and security risks to the network infrastructure. In this study, a phase-changing soft open point (PC-SOP) is proposed as a new way of connecting soft open points (SOPs) to balance the power flows among three phases by controlling active power and reactive power. Then an operational strategy based on PC-SOPs is presented for three-phase four-wire unbalanced systems. By optimising the regulation of SOPs, optimal energy storage systems dispatch and DG curtailment, the proposed strategy can reduce power losses and three-phase imbalance. Second-order cone programming (SOCP) relaxation is utilised to convert the original non-convex and non-linear model into an SOCP model which can be solved efficiently by commercial solvers. Case studies are conducted on a modified IEEE 34-node three-phase four-wire system and the IEEE 123-node test feeder to verify the effectiveness, efficiency and scalability of the proposed PC-SOP concept and its operational strategy.

Nomenclatures

γ^{VSC}	loss index of VSC
$VSCi$	VSC1, VSC2
φ	phase A, B or C
$P_{\varphi,t}^{\mathrm{VSC}i,\mathrm{loss}}$	active power loss of VSCi at phase φ at time t
$P_{\varphi,t}^{\mathrm{VSC}i}$	active power of VSCi at phase φ at time t
$Q_{\varphi,t}^{\mathrm{VSC}i}$	reactive power of VSCi at phase φ at time t
$S_{\varphi}^{\mathrm{VSC}i}$	capacity of VSCi at phase φ
$\boldsymbol{I}_{\mathrm{branch},t}$	$l \times 1$ vector containing all branch currents at time t
$\boldsymbol{R}$	$l \times 1$ vector containing all branch resistances
l	number of branches
$\boldsymbol{v}_t$	$n \times 1$ vector containing voltages at each node at time t
n	number of all nodes
m	number of buses, each bus have phase A, B, C and neutral nodes
$I_{\mathrm{branch,real},t}$	real part of $\boldsymbol{I}_{\mathrm{branch},t}$
$I_{\mathrm{branch,imag},t}$	imaginary part of $\boldsymbol{I}_{\mathrm{branch},t}$
$\mathrm{VUF}_{m,t}$	voltage unbalance factor at bus m at time t
$[\boldsymbol{Y}]$	$n \times n$ nodal admittance matrix
Y_i	nodal admittance at node i
$\boldsymbol{I}_{\mathrm{inj},t}$	$n \times 1$ vector containing all currents drawn or injected into the network at time t
$I_{\mathrm{inj},t}^{\mathrm{load}}$	current drawn by load at time t
$P_{i,t}^{\mathrm{load}}, Q_{i,t}^{\mathrm{load}}$	real and reactive load powers at node i at time t
$P_{i,t}^{\mathrm{DERs,\ SOPs\ or\ ESSs}}$	active powers of DERs, SOPs or ESSs at node i at time t
$Q_{i,t}^{\mathrm{DERs,\ SOPs\ or\ ESSs}}$	reactive powers of DERs, SOPs or ESSs at node i at time t
$I_{\mathrm{inj},t}^{DERs,\ SOPs\ \mathrm{or}\ ESSs}$	current contribution from DERs, SOPs or ESSs
$v_{i,t}$	voltage at node i at time t
$v_{i,\mathrm{real},t}, v_{i,\mathrm{imag},t}$	real part and imaginary part of $v_{i,t}$
$\overline{V_i}, \underline{V_i}$	maximum or minimum allowable steady-state voltage magnitude at node i
$V_{\varphi,m,t}$	phase φ voltages at bus m at time t
α	phasor rotation operator, $1\angle 120°$
Vi	nominal voltage at node i
$\boldsymbol{V}_{\mathrm{nominal}}$	$n \times 1$ vector containing nominal voltages at each node
V_{φ}	nominal network voltage at phase φ
$\overline{VUF_m}$	maximum allowable voltage unbalance factor at bus m
N	collection of neutral nodes
G_{ij}, B_{ij}	branch conductance and susceptance, respectively
$\overline{I_{ij}}$	current limit of branch connecting nodes i and j
$I_{ij,t}$	current of branch connecting nodes i and j at time t
$[\boldsymbol{M}]$	$l \times n$ connection matrix
$P_{i,t}^{\mathrm{ESS}}$	energy storage charging power or discharging power at node i at time t
$P_{i,t}^{\mathrm{ESS},c}, P_{i,t}^{\mathrm{ESS},d}$	energy storage charging power limit or discharging power limit at node i at time t
$E_{i,t}$	energy storage present state at node i
E_i^{ESS}	energy storage capacity at node i
$\mathrm{SOC}_{\min}, \mathrm{SOC}_{\max}$	minimum and maximum states of charge
$P_{i,t}^{\mathrm{MAX}}, Q_{i,t}^{\mathrm{MAX}}$	maximum active and maximum reactive powers of DER at node i at time t
$*$	conjugate transpose

1 Introduction

1.1 Three-phase imbalance in distribution networks

Three-phase imbalance commonly happens in around 70% of the UK's low voltage (LV) power distribution networks [1, 2]. Financial losses are incurred due to wire losses such as losses in neutral wires [3] and additional network reinforcement investment such as equipment failure caused by network unbalanced operation [4]. The conventional causes of imbalance are uneven load phase-allocations and randomness of single-phase load profiles [5–7]. Recently, the integration of various distributed energy resources

This is an open access article published by the IET under the Creative Commons Attribution License (http://creativecommons.org/licenses/by/3.0/)

(DERs) such as distributed generation (DG), plug-in electric vehicles (PEVs) and energy storage systems (ESSs) brings not only new opportunities but also challenges. For example, unbalanced three-phase voltages are observed more frequently because of increasing single-phase DER installations and uncertainties of renewable power generation outputs [8, 9] and charging/discharging of batteries and electric vehicles. However, the unbalance voltages can also be caused by other occurrences, e.g. (i) large single-phase distribution transformer; (ii) open phase of capacitor banks; (iii) open phase on the primary of a three-phase transformer; (iv) unequal transformer tap settings; (v) unequal impedances of the main feeders; (vi) faults or grounds in the power transformers, among others.

As a technique, single-phase loads can be moved from one phase to another when a definite maximum or minimum (or both) demand phase(s) can be found. Demand-side management as a technology from the view of managing load has been used for the above phase-balancing purpose [10]. However, the time variances of load and DG make the imbalance changing between phases. Therefore, over a given period of time, e.g. 24 h, there are no fixed maximum and minimum load phases. Various techniques are proposed from the angle of managing DGs and loads themselves. Jin *et al.* [11] optimised hierarchical power oscillations control for DG under unbalanced conditions. In [12], inclusion of voltage-dependency in current-injection based three-phase load flow is investigated and the results are compared with constant-power load model in terms of phase-balancing. Kaveh *et al.* [13] proposed a new technique based on bacterial foraging with spiral dynamic which is applied for simultaneously optimisation of re-phasing, reconfiguration and DG placement. In [14], smart distribution feeder was balanced by DG sizing and rephasing strategy simultaneously and the problem is investigated in deterministic and stochastic frameworks. Eftekhari and Sadegh [15] while introducing an optimal phase-balancing method, discussed the effect of load modelling on phase balancing studies. From an angle of changing the network itself, Borozan [16] reported an approach that reduces imbalance by distribution network reconfiguration with tie switches. However, the total switching operational time can be 1 to 100 s, by using tie switches to reconfigure the distribution networks [17]. To improve the switching performance, new types of switches with power-electronic devices, such as soft open points (SOPs), designed and installed to replace these traditional tie switches with much shorter response time (20 ms) [18], provide an alternative novel solution to flexible distribution networks.

In this paper, we have chosen to focus on the SOP-enabled network reconfiguration for alleviating three-phase imbalance.

1.2 Conventional SOPs

SOPs can control power flows to balance loads between feeders, reduce network losses and regulate voltage [19, 20]. Therefore, these operational performances can be improved by installing SOPs. In addition, issues from high penetration levels of DERs can be resolved. Generally, there are three basic topologies of SOPs: back-to-back voltage-source converter (B2B VSC), unified power flow controller, static synchronous series compensator [21]. Based on the B2B VSC topology, physical limits and power losses of the SOPs were considered [22]. In [23], a steady-state analysis framework was developed with a generic power injection model to quantify the operational benefits of a distribution network with SOPs under normal network operational conditions by using an improved Powell's direct set method. In [24], an assumption is proposed that if the compensator efficiency is improved beyond the determined boundary, zero net electrical losses can be achieved to be of further benefit to utilities. In [25], the authors present an algorithm that calculates the non-concurrent per-node demand and generation hosting capacity of a distribution network when adding an SOP to link two networks. To further exploit the benefits from SOPs, existing research has involved various aspects including distribution network planning, optimisation scheduling, operation control and fault recovery.

Distribution network planning: In [26, 27], researchers independently propose stochastic planning models with new control strategies or conventional assets such as demand-side response, coordinated voltage control, SOPs and the possibility of active power generation curtailment of the DG units. In [28], the authors formulate a mixed-integer non-linear programming (MINLP) model to optimally determine the locations and energy/power capacities of distributed ESSs in active distribution networks (ADNs) with SOPs. For the same purpose, in [29], considering the long-term operation characteristics of DG, an MINLP is formulated based on the typical operational scenarios generated by Wasserstein distance which can compare probability distributions.

Optimisation scheduling: In [30–32], optimisation problems, distribution network reconfiguration (DNR) and optimal SOP outputs are formulated simultaneously within a multi-objective framework, exploring the maximum DG penetration level that a distribution network can accommodate before violating the network operational constraints. In [33, 34], the authors propose an optimal operation of SOPs in ADNs under three-phase unbalanced conditions, and the flexible interconnection based on a multi-terminal SOP significantly benefits the operation of ADNs by using the second-order cone programming (SOCP)-based method. In [35], the authors propose an optimal reactive power control method for distribution systems with SOPs and consider the direct load control of thermostatically controlled air-conditioning. In [36], a two-stage adjustable robust optimisation model with operational strategies of SOP is built to tackle the uncertainties of photovoltaics (PV) outputs.

Operation control: The SOP based on direct modular multilevel converter is capable of bidirectional power flows between two feeders at any power factor, even when the feeders have different nominal voltages and operate with a phase-shift angle or unbalanced voltages [37]. In [18], the authors develop two control modes for the operation of the SOP. Under normal operational condition, the SOP can control real power and compensate reactive power. Under fault conditions, the SOP can effectively isolate fault zones. In [38], the authors use a Jacobian matrix-based sensitivity method to define the operational region of an SOP when the grids/feeders have various load and generation conditions. In [39], the authors consider the cooperation of SOPs and multiple voltage regulation devices and propose a coordinated real-time voltage and VAR control method based on the SOP for ADNs. The method converts the original non-convex mixed-integer non-linear optimisation model into a mixed-integer second-order cone program (MISOCP) model. In [40], the authors propose a decentralised voltage control strategy of SOPs in ADNs.

Fault recovery: In [41], the authors study the impact of using SOPs on an existing feeder automation scheme under balanced fault conditions. In [42], the authors use the primal–dual interior-point algorithm to solve the model of the supply restoration based on the SOP to improve the self-healing ability of the distribution system. In [43], the authors investigate the dynamic performance of a medium voltage (MV) distribution network with a connected SOP, under grid-side AC faults. The use of sequence networks is extended to include SOPs, such that conventional asymmetrical fault analysis technique can be used on a distribution network with SOPs.

Convex optimisation, especially SOCP and semidefinite programming (SDP), is widely used in research related to SOPs for mainly three reasons. First, the constraint of SOP, based on the B2B VSC topology, is a circle which is convex [19]. Second, although optimal power flow (OPF) problems, including single-phase OPF and three-phase OPF, are non-convex, it has been proved that the OPF problems can be converted into convex problems. Third, the intersection of convex sets is convex [44]. Therefore, most planning and optimisation scheduling service restoration problem of ADNs with SOPs can be converted into convex problems of power flows in ADNs with SOPs' constraints.

This is an open access article published by the IET under the Creative Commons Attribution License
(http://creativecommons.org/licenses/by/3.0/)

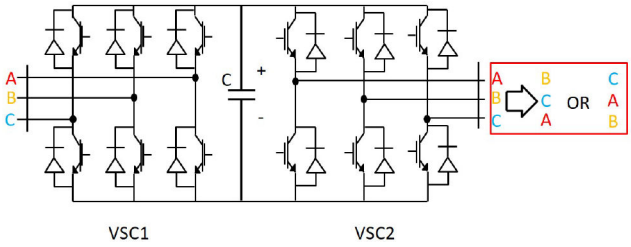

Fig. 1 *New ways of connection of the SOP (PC-SOP)*

1.3 Convex optimisation of power flows in ADNs

Research of convex optimisation of power flows in ADNs includes linear direct current optimal power-flow (DC OPF), single-phase OPF, three-phase OPF, robust control OPF and the exactness of the convex relaxation of OPF.

DC OPF: Although it can instruct economic dispatch, and consider the power flows with asset thermal constraints, DC OPF cannot be used for quantifying losses, voltage constraints or reactive power flows [45, 46] in most situations. In addition, DC approximations are more suitable for the transmission systems than the distribution systems [46]. Progresses have been made in this area: in [47], the authors explore the current–voltage (I–V) formulation of the power-flow problem and convexify a similar formulation for four-wire unbalanced distribution networks. Piecewise approximations with integer variables are proposed in [46, 48–50] by the application of Taylor expansions or similar to handle the non-convexity introduced by the quadratic losses. However, the computational burden is increased due to the increase of data with hundreds and thousands of dimensions. A linearly-constrained and convergence-guaranteed OPF method with reactive power and voltage calculations is proposed in [51] but the accuracy of the network model requires further improvement.

Single-phase OPF: In [52], the authors formulate the single-phase OPF in the distribution networks as a MISOCP, for which the global optimal solution up to the desired accuracy can be found by using available commercial solvers. The solutions proposed in this reference are proved not singular by the convergence of the Newton–Raphson solving scheme.

Three-phase OPF: The non-convexity of the single-phase OPF problem is much weaker than that of the three-phase OPF problem [53]. In [54], the authors develop a distributed SDP solver for the three-phase OPF problem based on the alternating direction method of multipliers and the Lagrangian relaxation method but with a near-global optimal solution of the relaxed problem. Algorithms proposed in [53] guarantee convergence and global optimality when the trace of the regularisation term becomes zero by combining the convex iteration method and the chordal-based conversion technique. In [55], the authors present a convex approximate AC OPF for unbalanced three-phase four-wire distribution networks with ESSs, especially when calculating power losses in the neutral wire and for meshed network configuration. The authors of [56, 57] report a three-phase OPF solution which was using the primal–dual interior point method and the three-phase current injection method in rectangular coordinates.

Robust control of OPF and relaxation exactness: Robust control algorithms are designed to deal with various challenges: load uncertainty – in [58], the authors propose a two-stage robust optimisation model for the DNR problem with load uncertainty. The model is solved by a column-and-constraint generation algorithm, in which the master problem and subproblem are transformed into an equivalent MISOCP. Complexity – in [59], the authors propose a quadratic programming model which can deal with the complexity due to the presence of discrete parameters and show the scalability and robustness of the proposed approach with improved or at least equal quality solutions for the problems. In addition, the exactness of the convex relaxation has been investigated in [60–62].

1.4 Summary and contributions of this paper

In summary, to improve the three-phase imbalance, with a solution of network reconfiguration using SOPs, focusing on the optimisation modelling, this paper proposes an optimised operational strategy for unbalanced ADNs based on SOPs and optimal ESSs dispatch, reducing the three-phase four-wire imbalances while enhancing the operational efficiency of ADNs. The contributions of this study are summarised as follows:

- The potential of SOPs is explored by a fresh way of connection, i.e. phase power transferring, so-called phase-changing SOP (PC-SOP).
- The benefits of PC-SOPs for unbalanced three-phase four-wire system are further analysed. A PC-SOP based optimal operational strategy for unbalanced ADNs is proposed considering power losses in the neutral wire.
- The OPF of three-phase four-wire imbalance system with SOPs is mathematically a non-convex non-linear problem. The original non-convex non-linear optimisation model is converted into an SOCP formulation, which can be efficiently solved to find the global optimum which can also meet the requirement of efficiency in problem solving.
- Demonstrated by a case study, by optimising the regulation of SOPs, optimal ESSs dispatch and PV curtailment, the reduction of energy losses and effective voltage regulation simultaneously achieved by the proposed approach are significant.

The paper is organised as follows: Section 2 is the unbalanced three-phase optimal operation problem formulation, in three-phase four-wire distribution systems; Section 3 presents the case study with four different cases for comparison and result analysis; Section 4 summarises the conclusion of the paper.

2 Unbalanced three-phase optimal operation problem formulation in three-phase four-wire distribution networks

2.1 Principles and modelling of PC-SOPs

Basic principles of SOPs: SOPs are power-electronic devices installed in ADNs to replace tie switches which can accurately and flexibly control power flows [38]. Therefore, ADNs with SOPs can operate with lower cable losses and lower risks caused by frequent switching actions. SOPs have capabilities to transfer active power, supply reactive power and achieve real-time control of voltage between the connected feeders. B2B VSCs are the most commonly used topology for commercial SOP in MV or LV networks. Three-phase active power and reactive power outputs can be controlled independently by SOPs based on the B2B VSC topology. These SOPs operate in a $PQ - V_{dc}Q$ control mode in normal conditions with a certain amount of device losses (the loss index of VSC is 0.00199 [42]). In a balanced system, three-phase feeders would be connected correspondingly (ABC to ABC).

Basic principles of PC-SOPs: However, considering the implementing principle of B2B VSC using a DC link to connect AC feeders, energy is transferred from AC to DC then back to AC. Thus, it is possible that different feeder phases can be connected which is beneficial for unbalanced systems. Energy will be shifted by SOPs from one phase of one feeder to another phase of another feeder.

As the DG outputs and electricity demand have randomness, there is always a mismatch between them. When they are distributed in different feeder phases, networks can achieve a better operating performance when all phases can be indirectly connected by SOPs. Therefore, new ways of connection of SOPs, called PC-SOP (ABC to BCA or CAB, marked by the red rectangle in Fig. 1) is proposed in this paper as shown.

The optimisation process will not affect or be affected by the control scheme and techniques such as various pulse-width modulation (PWM) technologies and their current controllers or controlling loops [18]. It is actually one of the advantages of using back-to-back converters, with a ‘decoupling DC-link’, in AC–AC

This is an open access article published by the IET under the Creative Commons Attribution License
(http://creativecommons.org/licenses/by/3.0/)

applications from high-power high-voltage, like HVDC tie-links between grids with different frequencies; to lower-power variable-speed, like doubly-fed induction generators for wind turbine power conversion systems; to here, the connection between one unbalanced feeder and another.

The optimisation model of PC-SOPs (using ABC to BCA as an example) is obtained with the following constraints:

PC-SOP active power constraints:

$$\begin{cases} P_{A,t}^{\mathrm{VSC1}} + P_{B,t}^{\mathrm{VSC2}} + P_{A,t}^{\mathrm{VSC1,loss}} + P_{B,t}^{\mathrm{VSC2,loss}} = 0, \\ P_{B,t}^{\mathrm{VSC1}} + P_{C,t}^{\mathrm{VSC2}} + P_{B,t}^{\mathrm{VSC1,loss}} + P_{C,t}^{\mathrm{VSC2,loss}} = 0, \\ P_{C,t}^{\mathrm{VSC1}} + P_{A,t}^{\mathrm{VSC2}} + P_{C,t}^{\mathrm{VSC1,loss}} + P_{A,t}^{\mathrm{VSC2,loss}} = 0 \end{cases} \tag{1}$$

$$P_{\varphi,t}^{\mathrm{VSC}i,\mathrm{loss}} = \gamma^{\mathrm{VSC}} \times P_{\varphi,t}^{\mathrm{VSC}i} \tag{2}$$

PC-SOP capacity constraint:

$$\sqrt{P_{\varphi,t}^{\mathrm{VSC}i^2} + Q_{\varphi,t}^{\mathrm{VSC}i^2}} \le S_{\varphi}^{\mathrm{VSC}i^2} \tag{3}$$

where $P_{\varphi,t}^{\mathrm{VSC}i}$ is the active power of VSCi at phase φ at time t, $Q_{\varphi,t}^{\mathrm{VSC}i}$ is the reactive power of VSCi at phase φ at time t and $S_{\varphi}^{\mathrm{VSC}i}$ is the capacity of VSCi at phase φ.

The SOP capacity constraint can be transferred into the SOCP model for optimisation

$$\| [P_{\varphi,t}^{\mathrm{VSC}i}, Q_{\varphi,t}^{\mathrm{VSC}i}] \|_2 \le S_{\varphi}^{\mathrm{VSC}i} \tag{4}$$

where $\| \ldots \|_2$ is the Euclidean norm [44] which is the standard form of the SOCP.

2.2 Modelling of three-phase four-wire ADNs with PVs, SOPs and ESSs

(1) Objective function: This paper proposes a linear weighted combination of minimum total power losses, the voltage deviation and the voltage unbalance condition

$$\min f = W_{\alpha} \times f^{\mathrm{loss}} + W_{\beta} \times f^{V,\mathrm{deviation}} + W_{\gamma} \times f^{VUF} \tag{5}$$

where W_{α}, W_{β} and W_{γ} are the wights for each factor and set as equally important (1.0 for each); f^{loss} is the power losses; $f^{V,\mathrm{deviation}}$ is the voltage deviation; f^{VUF} is the voltage unbalance condition. In addition, in real operations, engineers/researchers can set the weight factors considering their various requirements and priorities. Also, as a future work, recommended weighting factors can be proposed for defined situations, case by case.

Each function is formulated as follows:

$$f^{\mathrm{loss}} = \mathrm{sum}([I_{\mathrm{branch,real},t}^2 + I_{\mathrm{branch,imag},t}^2] \times R) \tag{6}$$

$$f^{V,\mathrm{deviation}} = \mathrm{sum}(\left| \boldsymbol{v}_t - V_{\mathrm{nominal}} \right|) \tag{7}$$

$$f^{\mathrm{VUF}} = \mathrm{sum}(\mathrm{VUF}_{m,t}) \tag{8}$$

where $\boldsymbol{I}_{\mathrm{branch},t}$ is an $l \times 1$ vector containing all branch currents at time t, with their real part $I_{\mathrm{branch,real},t}$ and imaginary part $I_{\mathrm{branch,imag},t}$; R, the vector containing all branch resistances; $\boldsymbol{v}_t$ is an $n \times 1$ vector containing voltages at each node at time t; $VUF_{m,t}$ is the voltage unbalance factor at bus m at time t; and V_{nominal} is an $n \times 1$ vector containing nominal voltages at each node.

(2) Three-phase four-wire system operational constraints:

Power flow constraints: This branch flow model is proposed for three-phase four-wire networks in [55]. It can be described mathematically with the following constraints. The nodal admittance matrix is the core of calculating power flows following Kirchhoff's current law [62] in this paper

$$[\boldsymbol{Y}]\boldsymbol{v}_t = \boldsymbol{I}_{\mathrm{inj},t} \tag{9}$$

where $[\boldsymbol{Y}]$ is the $n \times n$ nodal admittance matrix, $\boldsymbol{I}_{\mathrm{inj},t}$ is the $n \times 1$ vector containing all currents drawn or injected into the network at time t.

The loads, DERs, SOPs and ESSs are modelled as current injections

$$I_{\mathrm{inj},t}^{\mathrm{load}} = \frac{P_{i,t}^{\mathrm{load}} - j \times Q_{i,t}^{\mathrm{load}}}{V_i^*} \tag{10}$$

$$I_{\mathrm{inj},t}^{\mathrm{DERs,\ SOPs\ or\ ESSs}} = \frac{1}{V_i^*}(P_{i,t}^{\mathrm{DERs,\ SOPs\ or\ ESSs}} - j \times Q_{i,t}^{\mathrm{DERs,\ SOPs\ or\ ESSs}}) \tag{11}$$

$$\boldsymbol{I}_{\mathrm{inj},t} = \mathrm{sum}(I_{\mathrm{inj},t}^{\mathrm{DERs,\ SOPs\ or\ ESSs}}) - I_{\mathrm{inj},t}^{\mathrm{load}} \tag{12}$$

where $I_{\mathrm{inj},t}^{\mathrm{load}}$ is the current drawn by load at time t; $P_{i,t}^{\mathrm{load}}, Q_{i,t}^{\mathrm{load}}$ are the real and reactive load powers at node i at time t; $P_{i,t}^{\mathrm{DERs,\ SOPs\ or\ ESSs}}$ are the active powers of DERs, SOPs or ESSs at node i at time t; $Q_{i,t}^{\mathrm{DERs,\ SOPs\ or\ ESSs}}$ are the reactive powers of DERs, SOPs or ESSs at node i at time t; $I_{\mathrm{inj},t}^{\mathrm{DERs,\ SOPs\ or\ ESSs}}$ are the current contribution from DERs, SOPs or ESSs. Here V_i (nominal voltage at node i) are used to approximate the $v_{i,t}$ (variable, the voltage at node i at time t), because voltage deviations are relatively small compared with the changes of load, DERs, SOPs or ESSs.

For loss analysis, current sources are preferred for modelling purposes for loads, DERs and ESSs. In practice, although relatively few loads are constant current, a mixture of constant power and constant impedance loads often behaves like a constant current load. Therefore, constant current source is a reasonable approximation of a mixture of constant power and constant impedance loads. Moreover, the voltage deviations are small in magnitude compared to the actual voltage values. The accuracy of constant current modelling of loads and DGs have been proved mathematically and practically in [55] with reasonable errors of voltages and currents up to 0.2 and 2%, respectively.

Voltage limits: Each bus voltage can be expressed as a linear combination of the injected currents

$$\begin{aligned} v_{i,\mathrm{real},t} = {} & Re([Y_i^*]^{-1}) \times I_{\mathrm{inj,real},t} \\ & - Im([Y_i^*]^{-1}) \times I_{\mathrm{inj,imag},t} \end{aligned} \tag{13}$$

$$\begin{aligned} v_{i,\mathrm{imag},t} = {} & Re([Y_i^*]^{-1}) \times I_{\mathrm{inj,real},t} \\ & + Im([Y_i^*]^{-1}) \times I_{\mathrm{inj,imag},t} \end{aligned} \tag{14}$$

$$v_{i,\mathrm{real},t}^2 + v_{i,\mathrm{imag},t}^2 \le \overline{V_i}^2 \tag{15}$$

$$-K_{1A}v_{i,\mathrm{real},t} - K_{2A}v_{i,\mathrm{imag},t} \le -\underline{V_i}, \quad i \in \text{phase } A \tag{16}$$

$$-K_{1B}v_{i,\mathrm{real},t} - K_{2B}v_{i,\mathrm{imag},t} \le -\underline{V_i}, \quad i \in \text{phase } B \tag{17}$$

$$-K_{1C}v_{i,\mathrm{real},t} - K_{2C}v_{i,\mathrm{imag},t} \le -\underline{V_i}, \quad i \in \text{phase } C \tag{18}$$

where $v_{i,\mathrm{real},t}, v_{i,\mathrm{imag},t}$ are the real part and imaginary part of $v_{i,t}$; $\overline{V_i}$, $\underline{V_i}$ are the maximum and minimum allowable steady-state voltage magnitudes at node i.

Based on the fact that the approximate voltage angle is known at all phase nodes, the constants $K_{1A}, K_{2A}, K_{1B}, K_{2B}, K_{1C}, K_{2C}$ can be chosen to minimise the weighted average squared approximation error over an angle deviation of 10 degrees from the approximate voltage angle [63].

Voltage imbalance constraints:

This is an open access article published by the IET under the Creative Commons Attribution License (http://creativecommons.org/licenses/by/3.0/)

$$\mathrm{VUF}_{m,t} = \frac{V_{A,m,t} + \alpha^2 V_{B,m,t} + \alpha V_{C,m,t}}{V_{A,m,t} + \alpha V_{B,m,t} + \alpha^2 V_{C,m,t}} \simeq \frac{V_{A,m,t} + \alpha^2 V_{B,m,t} + \alpha V_{C,m,t}}{V_{\varphi}} \tag{19}$$

$$\mathrm{VUF}_{m,t}^2 \leq \overline{\mathrm{VUF}_m}^2 \tag{20}$$

where $V_{\varphi,m,t}$ is the phase φ voltages at bus m at time t; α is the phasor rotation operator, $1\angle 120°$; $\overline{\mathrm{VUF}_m}$ is the maximum allowable voltage unbalance factor at bus m.

Current limits: The current through a branch connecting nodes i and j is then

$$\left|I_{ij,t}\right| = \sqrt{(G_{ij}^2 + B_{ij}^2)} \times \sqrt{(v_{i,\mathrm{real},t} - v_{j,\mathrm{real},t})^2 + (v_{i,\mathrm{imag},t} - v_{j,\mathrm{imag},t})^2} \tag{21}$$

and

$$\left|I_{ij,t}\right|^2 \leq \overline{I_{ij}}^2 \tag{22}$$

where $I_{ij,t}$ is the current of branch connecting nodes i and j at time t; G_{ij}, B_{ij} are the branch conductance and susceptance, respectively; $\overline{I_{ij}}$ is the current limit of the branch connecting nodes i and j [64].

Then the above model can be converted to an SOCP model

$$\sqrt{(G_{ij}^2 + B_{ij}^2)} \parallel [(v_{i,\mathrm{real},t} - v_{j,\mathrm{real},t}), (v_{i,\mathrm{imag},t} - v_{j,\mathrm{imag},t}] \parallel_2 \leq \left|\overline{I_{ij}}\right| \tag{23}$$

Branch current limits:

$$\boldsymbol{I}_{\mathrm{branch},t} = [\boldsymbol{M}]v_t = [\boldsymbol{M}][\boldsymbol{Y}]^{-1}\boldsymbol{I}_{\mathrm{inj},t} \tag{24}$$

where $[\boldsymbol{M}]$ is the $l \times n$ connection matrix.

Constraints of energy storage:

$$\begin{cases} E_{i,t} = E_{i,t-1} + P_{i,t}^{\mathrm{ESS}} \; i \in \text{ phase A, B or C} \\ \left|P_{i,t}^{\mathrm{ESS},c}\right| \leq \left|P_{i,t}^{\mathrm{ESS}}\right| \leq \left|P_{i,t}^{\mathrm{ESS},d}\right| \\ E_i^{\mathrm{ESS}} SOC_{\min} \leq E_{i,t} \leq E_i^{\mathrm{ESS}} \mathrm{SOC}_{\max} \end{cases} \tag{25}$$

where $P_{i,t}^{\mathrm{ESS}}$ is the energy storage charging power or discharging power at node i at time t; $P_{i,t}^{\mathrm{ESS},c}$, $P_{i,t}^{\mathrm{ESS},d}$ are the energy storage charging and discharging power limits at node i at time t; $E_{i,t}$ is the energy storage present state at node i; E_i^{ESS} is the energy storage capacity at node i; $\mathrm{SOC}_{\min}$, $\mathrm{SOC}_{\max}$ are the minimum and maximum states of charge.

Constraints of DER output:

$$\begin{cases} 0 \leq P_{i,t}^{\mathrm{DER}} \leq P_{i,t}^{\mathrm{MAX}} \\ 0 \leq Q_{i,t}^{\mathrm{DER}} \leq Q_{i,t}^{\mathrm{MAX}} \; i \in \text{ phase A, B or C} \end{cases} \tag{26}$$

where $P_{i,t}^{\mathrm{MAX}}$, $Q_{i,t}^{\mathrm{MAX}}$ are the maximum active and reactive powers of DER at node i at time t.

The detailed procedure of implementing the proposed model and algorithms is shown in Fig. 2. After the input of data such as network parameters, load profiles, ESS profiles and PC-SOP locations and sizes, the SOCP problem is relaxed for PC-SOP and the power flow constraints. As ESSs are some of the controllable variables with important initial status, they are assigned with specific constraints. Then the optimisation can be solved as an SOCP OPF problem with power flows and variables considered for a 24 h simulation period, coded in Gurobi.

3 Case study

In this section, a modified IEEE 34-node test feeder (line voltage 24.9 kV) as shown in Fig. 3*a* is used as a test system to analyse and verify the proposed model [65, 66]. Data of the IEEE 34-node test feeder is presented in Tables 1 and 2 (for other data, one can also refer to [66].). The calculation process of the original fourth-order matrices of four-wire configurations is shown in [67]. To demonstrate the proposed model, the system is modified by removing all regulators and transformers. Single-phase overhead line configurations 302, 303 and 304 are replaced by three-phase overhead line configuration 300. The transformer between 832 and 888 is replaced by a 10 ft 301 configuration. Residential loads are in the dashed-border block, and other loads are commercial. The capacity of the SOP is 100 kVA and they are located between buses 822 and 848. The voltage range of all buses is set to be [0.94, 1.10] as the statutory limits in the UK [68]. The DERs (include PVs and ESSs) are required to operate with a fixed power factor of 0.95. Specifically, the ANSI standard recommends that the electric supply system should be made and function to limit the maximum voltage unbalance to 3% [69]. Four PVs are installed at buses 806 (three-phase, 300 kW), 818 (phase C, 300 kW), 820 (phase C, 600 kW) and 822 (phase C, 600 kW). Four ESSs are installed at buses 842 (three-phase, 100 kW), 844 (phase A, 400 kW), 846 (phase A, 400 kW) and 848 (three-phase, 400 kW). The initial state of charge (SOC) of all ESSs is fixed as 0.5, with a minimum of 0.2 and a maximum of 0.8.

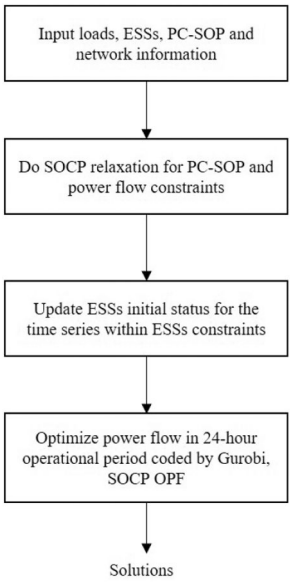

Fig. 2 *Flow chart of the applied solving process with the proposed model and algorithms*

The SOCP program proposed in this paper is coded by YALMIP [70], and solved by Gurobi [71]. The solving process is the primal–dual interior-point method which is a general process of how the solver solves SOCP problem, including: (i) finding the dual SOCP, (ii) defining barrier for second-order cone, (iii) defining primal–dual potential function, (iv) finding strictly feasible initial points and (v) using primal–dual potential reduction algorithm [44]. The proposed optimisation method is implemented with MATLAB R2019a, and the operating environment is Intel i5-5200 2.2 GHz CPU, 8GB RAM.

In this paper, four types of 'imbalances' are classified in the test system as shown in Fig. 3*b*.

- Peak time imbalance for the three phases: Loads in the residential area (around hour 7 and around hour 17) and the commercial area (hour 9 to hour 21) have different peak hours.
- Total load amount imbalance for the three phases: Loads in phases A, B and C have different total amount for power (456, 418 and 429 kW at hour 1). Meanwhile, loads in phase A (169 kW) are higher than phase B (72.5 kW) and phase C (27 kW) in the residential area at the hour 1. Conversely, loads in phases C (402 kW) are higher than phase A (287 kW) and phase B (345.5 kW) in the commercial area at the hour 1. In addition, loads in phase A in the residential area and loads in phase C in the

This is an open access article published by the IET under the Creative Commons Attribution License (http://creativecommons.org/licenses/by/3.0/)

commercial area are higher than other phases in following hours.

- Location imbalance for different phase loads: Except the highest three load demand at bus 846, loads in phases A, B and C have different power distribution. In phase A, the second highest load demand is close to the middle of the feeder (bus 832). In phase B, loads are distributed evenly. In phase C, the second highest load demand is close to the end of the feeder (bus 864).
- Loads and DGs imbalance: In the residential area, the total power of phase A is higher than those of phase B and phase C. However, the single-phase PVs are allocated in phase B. In the commercial area, the total power of phase C is higher than those of phase A and phase B. However, the single-phase ESSs are allocated in phase B.

Two different connections of PC-SOP are compared with optimisation results in Table 3. PC-SOP (ABC to BAC) results in less PV curtailment. In contrast, PC-SOP (ABC to CAB) achieves better network performance in terms of power losses and three-phase voltage unbalance condition. In general, although these PC-SOPs with different ways of connection have individual advantages in the optimisation results, the absolute deviations between them are negligible. Therefore, here we choose the PC-SOP (ABC to BAC) to represent the PC-SOP solution for comparison with other solutions.

Four cases are designed to show the benefits of PC-SOP and coordinated optimsation of PC-SOP and ESSs.

Case 1: the system with PC-SOP and ESSs.
Case 2: the system with conventional SOP and ESSs.
Case 3: the system with SVCs and ESSs as shown in Fig. 4. (The same capacity SVCs are used to replace SOP.)
Case 4: the system with only ESSs.

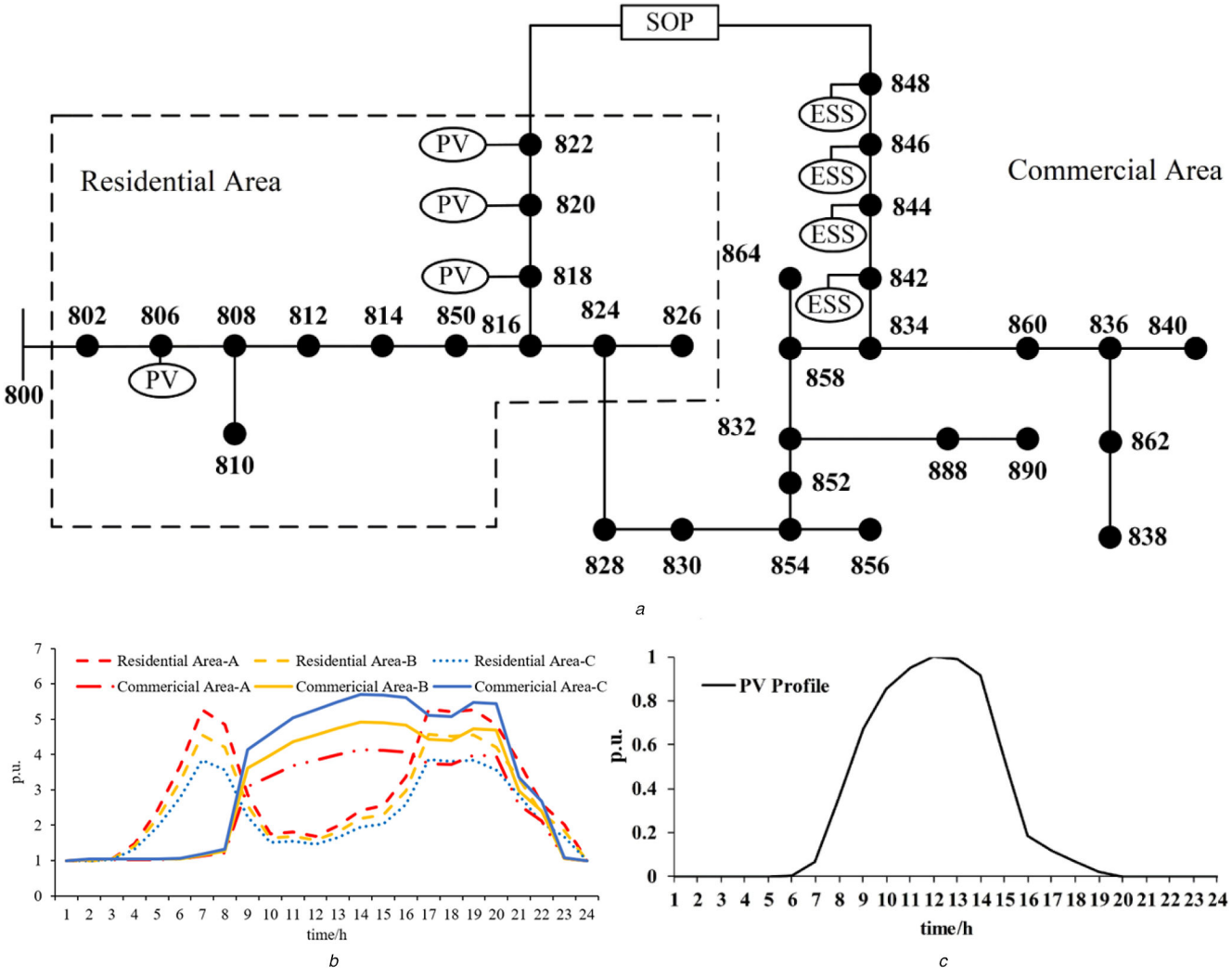

Fig. 3 *Modified IEEE 34-node test feeder*
(a) Topology of the modified system, ***(b)*** Residential area and commercial area profiles, ***(c)*** Individual PV generation profile

Table 1 Spot loads of the IEEE 34-node test feeder

Node	Ph-1 kW	Ph-1 kVAr	Ph-2 kW	Ph-2 kVAr	Ph-3 kW	Ph-3 kVAr
860	20	16	20	16	20	16
840	9	7	9	7	9	7
844	135	105	135	105	135	105
848	20	16	20	16	20	16
890	150	75	150	75	150	75
830	10	5	10	5	25	10
Total	344	224	344	224	359	229

This is an open access article published by the IET under the Creative Commons Attribution License (http://creativecommons.org/licenses/by/3.0/)

The results in Table 4 show that the PC-SOP (Case 1) can reduce network losses and PV curtailment – all network losses, neutral wire losses and PV curtailment are the lowest (3527.77, 382.99 and 1208.91 kW/24 h, respectively). Especially neutral wire loss has the lowest percentage (10.86%) among four cases. Meanwhile, the PC-SOP can considerably reduce voltage deviation and three-phase voltage unbalance condition (+0.50/ − 0.60 and 1.63%, respectively). In other cases, the minimum value of voltages drop out of constraints [0.94,1.10]. Compared with Case 4, the conventional SOP (Case 2) or SVCs (Case 3) can also reduce network losses and improve PV integration. The PC-SOP helps achieve optimised results and best performance of the distribution network among all four cases. It is worth noting that the maximum neutral wire current among the four cases is 54.1 A, which is much lower than the normal phases (maximum 236.72 A), hence not considered as critical constraints.

Table 2 Distributed loads of the IEEE 34-node test feeder

Node A	Node B	Ph-1 kW	Ph-1 kVAr	Ph-2 kW	Ph-2 kVAr	Ph-3 kW	Ph-3 kVAr
802	806	0	0	30	15	25	14
808	810	0	0	16	8	0	0
818	820	34	17	0	0	0	0
820	822	135	70	0	0	0	0
816	824	0	0	5	2	0	0
824	826	0	0	40	20	0	0
824	828	0	0	0	0	4	2
828	830	7	3	0	0	0	0
854	856	0	0	4	2	0	0
832	858	7	3	2	1	6	3
858	864	2	1	0	0	0	0
858	834	4	2	15	8	13	7
834	860	16	8	20	10	110	55
860	836	30	15	10	6	42	22
836	840	18	9	22	11	0	0
862	838	0	0	28	14	0	0
842	844	9	5	0	0	0	0
844	846	0	0	25	12	20	11
846	848	0	0	23	11	0	0
Total		262	133	240	120	220	114

This will be discussed in detail from four aspects: active power controlled by SOP (Section 3.1), PV curtailment and ESSs utilisation (Section 3.2), reactive power compensation by SOP and voltage profile (Section 3.3) and algorithm validation (Section 3.4).

3.1 Active power controlled by the PC-SOP

The PC-SOP, compared with the conventional SOP, can transfer more power and utilise the network capacity better in unbalanced systems. It can provide links between loads and DGs in different phases, as shown in Fig. 5. Differences in transmitted power between the PC-SOP and the SOP are analysed in detail as follows:

- In general, power is transferred from the residential area to the commercial area because PVs are installed in the residential area for both Case 1 and Case 2.
- The operational power of the PC-SOP is greater than that of the SOP. The average active power of the PC-SOP is 186.81 kW. The average active power of the conventional SOP is 183.29 kW.
- When the residential area loads achieve peak value at hour 7 (especially phase A), the PC-SOP can transfer power from the commercial area to the residential area while the conventional SOP cannot achieve that. This explains why there is bi-directional power transfer in Case 1 between 822 phase A and 848 phase B (shown as the green arrow in Fig. 5*c*).

3.2 PV curtailment and ESS utilisation

PV curtailment: In Fig. 6, Case 1 shows maximised PV outputs for all installed locations, while Case 4 shows the overall minimal. For three-phase PV 806 and single-phase PV 818, there is nearly no PV curtailment in all four cases. This is due to that these PVs are on or close to the main system's wire. PVs 820 and 822 hardly generate power which ranges from 0 to 300 kW in Cases 2, 3 and 4. However, the PC-SOP in Case 1 can make the system effectively utilise different phase resources – the outputs of all PVs 820 and 822 in Case 1 exceed 400 kW, because the PC-SOP effectively acts as a bridge to provide a path of power transfer between DGs and loads from different phases (between PVs in phase B and the highest load demand in the commercial area in phase C).

ESS utilisation: ESSs in combination with the PC-SOP can achieve the power regulation by shifting ESS charging or discharging meanwhile the PC-SOP can accomplish the spatial

Table 3 Comparison of different connection ways of PC-SOP

	Network losses (kW/24h)	Neutral wire losss (kW/24h)	Neutral wire loss proportion[a]	PV cutailment (kW/ 24h)	Voltage deviation	Three-phase voltage unbalance condition
PC-SOP (BAC)	3527.77	382.86	10.85%	1208.91	+0.50%/ − 0.60%	1.63%
PC-SOP (CAB)	3509.20	379.34	10.81%	1296.23	+0.50%/ − 0.60%	1.62%

[a] Neutral wire loss proportion = Neutral wire loss / Network loss

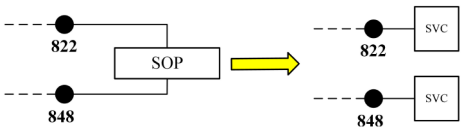

Fig. 4 *Concept of using SVCs to replace the SOP with the same capacity*

Table 4 Optimisation results comparison

	Network losses (kW/24h)	Neutral wire losss (kW/24h)	Neutral wire loss Proportion	PV cutailment (kW/ 24h)	Voltage deviation	Three-phase voltage unbalance condition
Case 1	3527.77	382.86	10.86%	1208.91	+0.50%/ − 0.60%	1.63%
Case 2	3723.85	735.67	19.76%	3449.77	+0.50%/ − 0.62%	2.53%
Case 3	3984.33	681.59	17.11%	4649.51	+0.5%/ − 0.63%	2.43%
Case 4	4690.74	990.58	21.12%	5580.13	+0.5%/ − 0.76%	3.03 %

This is an open access article published by the IET under the Creative Commons Attribution License (http://creativecommons.org/licenses/by/3.0/)

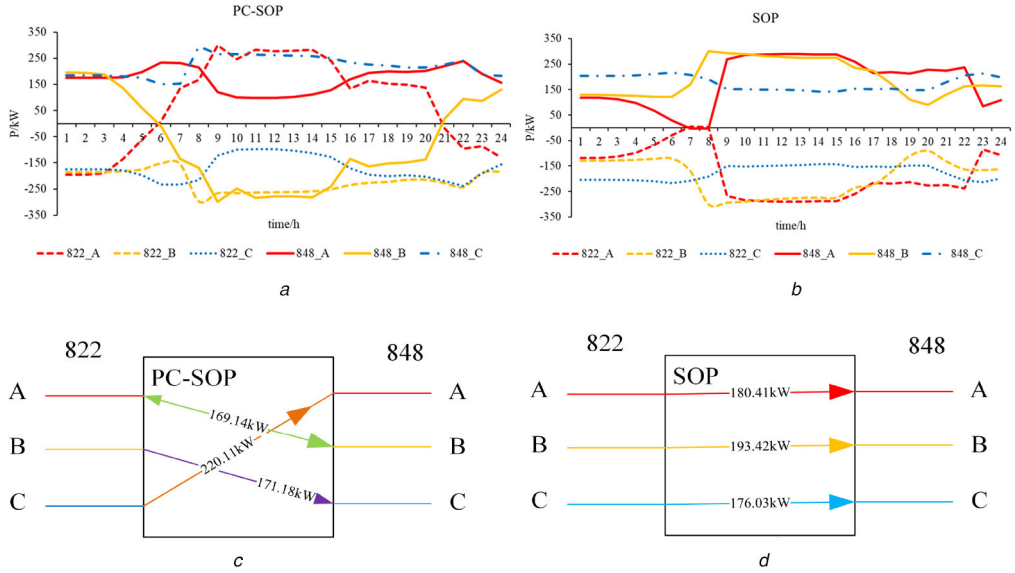

Fig. 5 *SOP active power outcome of Case 1*

(a) PC-SOP active power outcome, ***(b)*** SOP active power outcome, ***(c)*** PC-SOP average active power outcome, ***(d)*** SOP average active power outcome

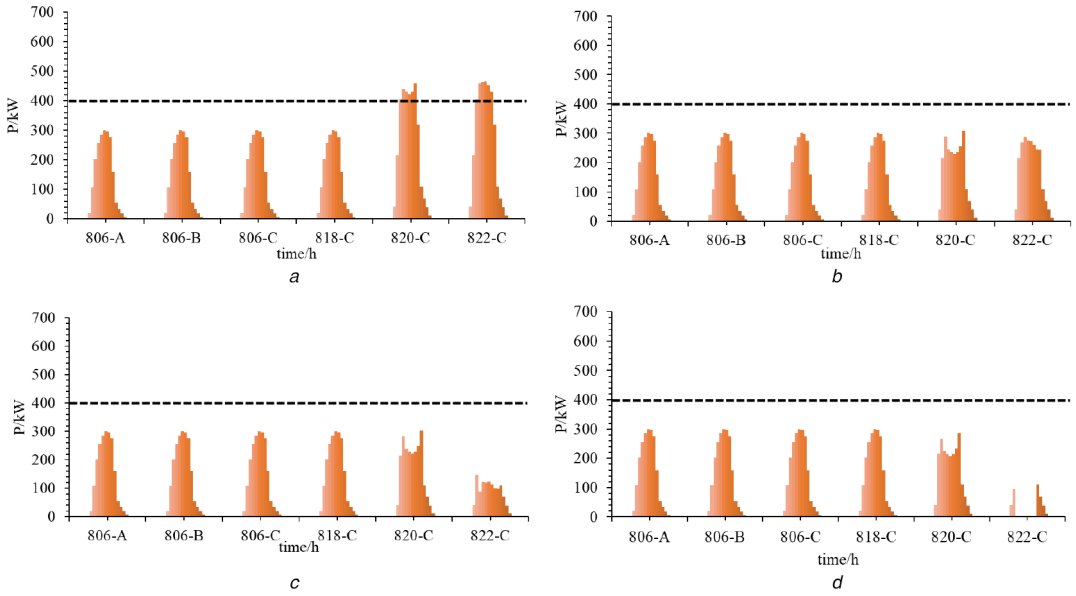

Fig. 6 *Actual PV outputs*

(a) Case 1, ***(b)*** Case 2, ***(c)*** Case 3, ***(d)*** Case 4

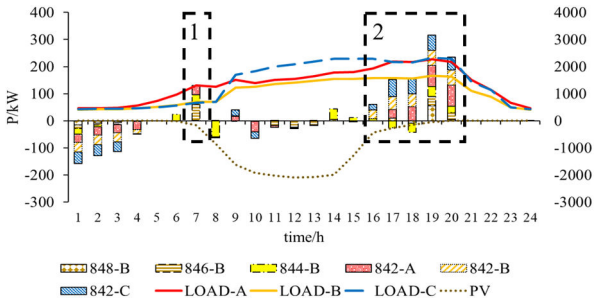

Fig. 7 *ESS output profiles*

power transfer between different phases by flexibly connecting different phases from adjacent feeders in Fig. 7.

In Period 1 (hour 1 to hour 5), load demand is relatively low and ESSs store energy.

In Period 2 (hour 6 to hour 16), ESSs output power at hour 7 (dashed square 1) because phase A demand is high in the residential area. ESSs output power not only in phase A (842-A) but also in phase B (848-B and 844-B). ESSs in phase B are also linked to loads in phase A by the PC-SOP. Due to the PC-SOP, PV's output power in phase B is directly transferred to other phase loads. Therefore, ESSs did not need to store a lot of energy from hour 8 to hour 16.

In Period 3 (hour 17 to hour 20), ESSs output power is the highest, because PVs stop to output at night when load demands are still high (dashed square 2).

In Period 4 (after hour 20), load demands decrease and ESSs stop outputing power .

3.3 Reactive power compensation and voltage profile

Reactive power compensation: The PC-SOP can achieve better voltage profiles and reduce three-phase voltage imbalance in Case 1 than those in Cases 2 and 3 with less reactive power support, as shown in Figs. 8 and 9. That means the PC-SOP's capacity is better utilised for transferring active power. Meanwhile, the PC-SOP sees less reactive power (maximum output not above 1400 kVar) in the system than SOP (maximum output between 1400 and 1600 kVar) and SVC (maximum output above 1600 kVar). Meanwhile, experimental data illustrates that the system with the PC-SOP can use PVs' reactive power (4414.70 kVar) more than other cases (4056.46, 2982.98 and 3208.04 kVar). Therefore, systems with the

This is an open access article published by the IET under the Creative Commons Attribution License (http://creativecommons.org/licenses/by/3.0/)

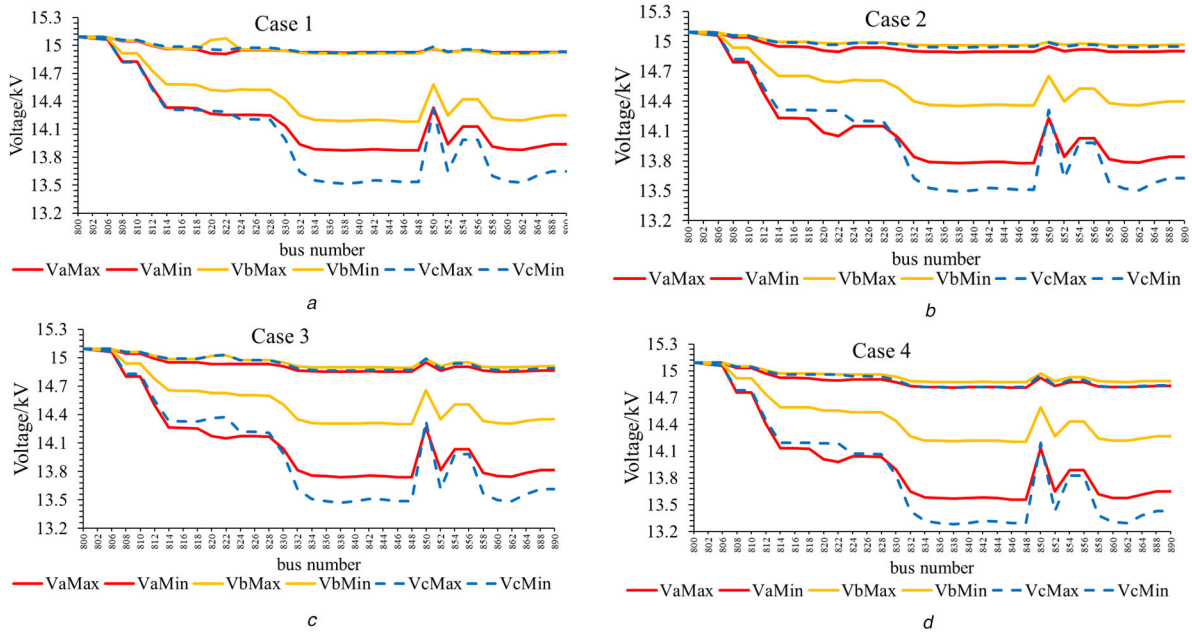

Fig. 8 *Maximum and minimum voltage of three phases*
(a) Case 1, ***(b)*** Case 2, ***(c)*** Case 3, ***(d)*** Case 4

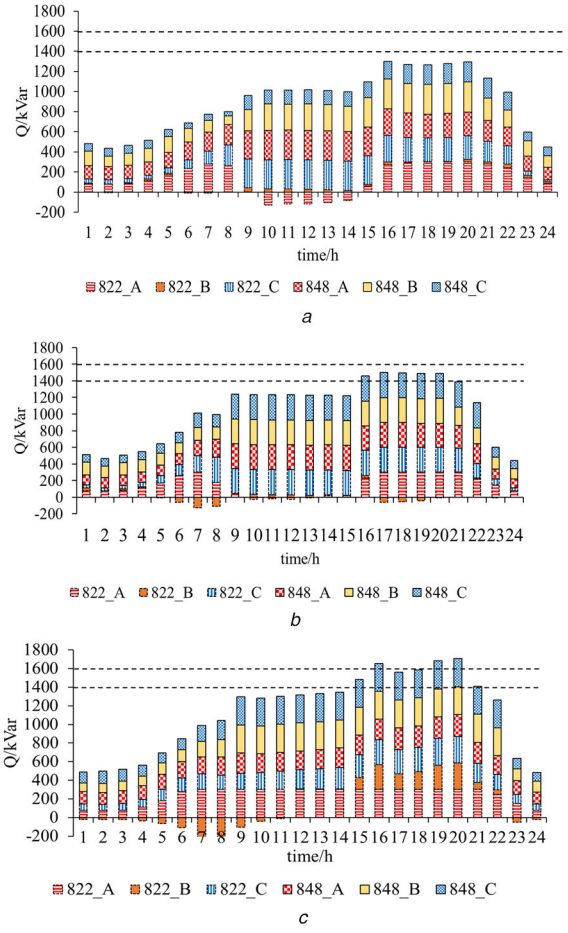

Fig. 9 *Reactive power outcomes*
(a) PC-SOP reactive power of Case 1, ***(b)*** SOP reactive power of Case 2, ***(c)*** SVC reactive power of Case 3

PC-SOP can utilise PVs' reactive power better and leave more capacities for the PC-SOP to transfer active power.

Voltage profile: In Case 1, no bus voltage is lower than 13.5134 kV ($\underline{V}_i$, minimum statutory limit of 94%). In Case 2, Case 3 and Case 4, there are 6 buses, 10 buses and 16 buses whose voltages are lower than 13.5134 kV ($\underline{V}_i$) during the 24 h operational period, respectively. By comparing Case 1 and Case 4 in Fig. 8, it can be seen that the PC-SOP did not make the operation of any other buses deteriorate. Instead, it improves all bus voltages: not only the voltages at buses 822 and 848 (where the PC-SOP is connected in between), but also the voltages at other buses (minimum voltage buses over 24 h, i.e. in Case 4, 832, 834, 836, 838, 840, 842, 844, 846, 848, 852, 858, 860, 862, 864, 888, 890, which are the majority of the commercial area buses; the other four buses 828, 830, 854, 856 are the buses close to the residential area and their voltages are above 94%). Thus, by connecting the PC-SOP, the transferring of unbalanced power improves voltage performance not only at buses near PC-SOP but also at all other buses, to ensure the system voltages at all buses are always within the statutory limits specified.

3.4 Algorithm validation

(1) Algorithm accuracy validation

The computation information of the four cases is shown in Table 5. It can be seen that the maximum deviation of convex relaxation converges to the predefined calculation precision (1×10^{-8}p.u.) in around 15 iterations. Thus, the SOCP-based approach calculates distribution system power flow with the PC-SOP with acceptable accuracy. Here, IPOPT (Interior Point OPTimiser) is also used to solve the same instances again to verify the accuracy and efficiency of the proposed method. IPOPT is a software library for large-scale non-linear optimisation of continuous systems [72]. It can be observed that the proposed method obtains the desirable solution of the flexibility evaluation problem with an improved computational efficiency, compared with the IPOPT package. Due to the convexification and the proper relaxation of the original problem, the SOCP-based method reduces the solving complexity (within 36 s) and obtains the solutions with a reasonable accuracy. This creates possibilities for modelling larger test feeders (e.g. IEEE 8500-node test feeder).

2) Algorithm scalability validation

In [34], the IEEE 123-node distribution system is used to verify the scalability of the optimal operation of conventional SOPs on large-scale ADNs with severe unbalanced conditions. Results show that regulating the operation of SOPs in ADNs can reduce power losses, mitigate three-phase unbalanced condition and effectively mitigate each phase voltage deviation from the nominal value to improve the voltage profile compared with cases without SOP.

To cross compare the results and benefits, here the proposed PC-SOP is analysed further with the same system, capacities of SOPs and allocation of PVs. The way of connection under analysis

This is an open access article published by the IET under the Creative Commons Attribution License
(http://creativecommons.org/licenses/by/3.0/)

Table 5 Computation information of the four cases and performance comparison between the proposed method and IPOPT

Case	Proposed method				IPOPT	
	Iteration steps	Gap, p.u.	Evaluation index[a]	Time, s	Evaluation index[a]	Time, s
1	16	1.37E-08	3527.77	34.835	3527.77	368.489
2	17	8.98E-10	3723.85	35.176	3723.86	356.376
3	15	2.76E-09	3984.33	35.850	3984.33	362.182
4	15	4.23E-12	4690.74	27.083	4690.74	256.200

[a]Evaluation index - total power loss f^{loss}.

Table 6 Optimisation results of the four scenarios with IEEE 123-node test feeder

Scenario	Power losses for three phase, kW	Power losses for neutral wire, kW	Three-phase unbalance condition	Voltage deviation	Time, s	IPOPT power losses for three-phase, kW	IPOPT Time, s
I	93.84	10.66	0.08%	0%/ – 0.35%	1.54	93.84	14.52
II	67.29	8.32	0.12%	0%/ – 0.22%	1.44	67.29	13.59
III	80.08	6.47	0.07%	0%/ – 0.30%	1.33	80.08	12.47
IV	63.93	6.02	0.10%	0%/ – 0.19%	1.32	63.93	12.47

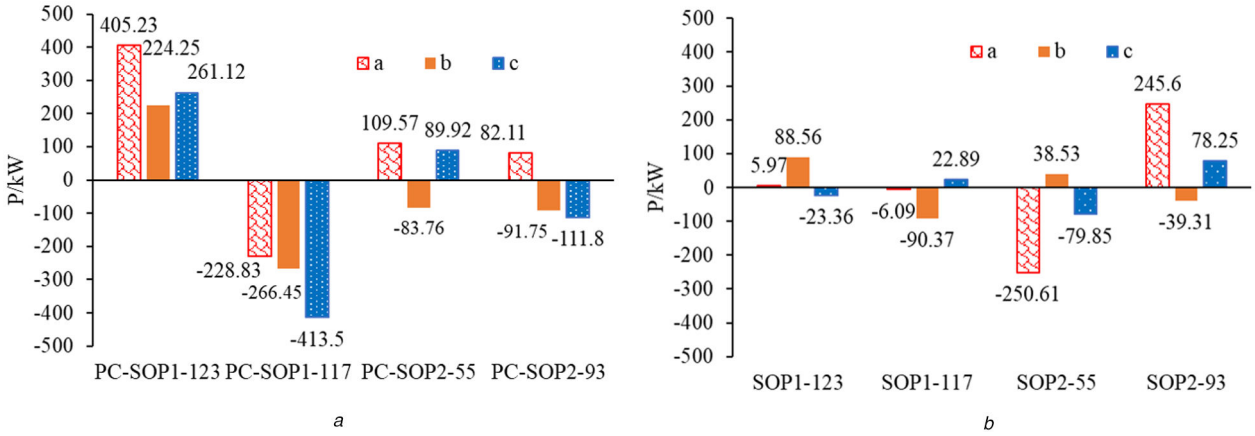

Fig. 10 *Comparison of active power outputs of SOP and PC-SOP*
(a) Three-phase active power outputs of PC-SOP, ***(b)*** Three-phase active power outputs of SOP

of two PC-SOPs is ABC to CAB. Four scenarios are analysed and compared as follows:

Scenario I: No PV integration in the system, the unbalanced optimal operation is conducted based on SOPs ('Scenario II' in [34]).
Scenario II: Considering 60% penetration of PVs, the unbalanced optimal operation is conducted based on SOPs ('Scenario IV' in [34]).
Scenario III: No PV integration in the system, the unbalanced optimal operation is conducted based on PC-SOPs.
Scenario IV: Considering 60% penetration of PVs, the unbalanced optimal operation is conducted based on PC-SOPs.

Comparison results in Table 6 show that, for both scenarios with and without unbalanced DG (PVs), PC-SOP has consistent benefits in all aspects: reducing power losses (i.e. from 93.84 to 80.08 kW, and from 67.29 to 63.93 kW, respectively), three-phase unbalance condition (from 0.08 to 0.07%, and from 0.12 to 0.10%) and voltage deviation (from 0.35 to 0.30%, and from 0.22 to 0.19%), compared with conventional SOP. The reason in essence is that PC-SOP can transmit more active power and unitise its capacity better than conventional SOP (from below 300 to up to 400 kW), as shown in Fig. 10.

In addition, the computation efficiency and robustness of the proposed method are checked again by comparing results with IPOPT in Table 6. The simulation speeds of the implementations again are consistently improved compared with IPOPT from minimum 12.47 to 1.32 s. Moreover, it makes not much difference in simulating difference scenarios of SOPs and PC-SOPs.

As shown from the above results and analysis, by optimising the operations of the PC-SOP and ESSs, OPF of the three-phase active and reactive power of the system can be achieved. Unbalanced condition is further improved, and the operational losses are further decreased by the PC-SOP compared with the conventional SOP and SVCs in both the IEEE 34-node and the 123-node test feeders.

4 Conclusion

This paper presents a new way of SOP connections called PC-SOP. An optimised operational strategy based on PC-SOPs is proposed to minimise the operational losses, three-phase imbalances, considering growing penetration levels of DERs for unbalanced three-phase four-wire distribution networks. Compared with conventional SOPs and SVCs, the optimisation results indicate that PC-SOPs significantly reduce unbalanced loading condition and power losses (especially neutral wire losses) in ADNs. PC-SOP can also make improved use of ESSs in unbalanced systems by transferring power between different phases. Furthermore, the proposed approach can provide support during the planning and installation stages, with a new solution and concept of PC-SOP, especially when it is required to improve unbalanced loading conditions. For system operators, it can help to achieve a 24 h optimal plan of ADNs with the addition of flexible and controllable resources such as PC-SOPs, PVs and ESSs in smart distribution systems. For three-phase imbalance in ADNs, the coordination and time-response between PC-SOP and other phase transferring techniques require further research, taking into account the robustness of the three-phase imbalance system optimisation and capital investment of power-electronic switches.

This is an open access article published by the IET under the Creative Commons Attribution License (http://creativecommons.org/licenses/by/3.0/)

5 Acknowledgments

The work is supported by projects 'Electricity Satnav – electricity smart availability topology of network for abundant electric vehicles' (Reference: EP/R001456/2), and 'Street2Grid – an electricity blockchain platform for P2P energy trading' (Reference: EP/S001778/2), which are funded by the Engineering and Physical Sciences Research Council (EPSRC), UK. Chengwei Lou thanks the China Scholarship Council (CSC201806350260) and the University of Glasgow for supporting his PhD study.

6 References

[1] Ma, K., Li, R., Li, F.: 'Utility-scale estimation of additional reinforcement cost from three-phase imbalance considering thermal constraints', *IEEE Trans. Power Syst.*, 2017, **32**, (5), pp. 3912–3923

[2] Kong, W., Ma, K., Wu, Q.: 'Three-phase power imbalance decomposition into systematic imbalance and random imbalance', *IEEE Trans. Power Syst.*, 2018, **33**, (3), pp. 3001–3012

[3] Distribution, E., Losses, S., Overview, N.t.: 'Electricity Distribution Systems Losses Non-Technical Overview A paper prepared for Ofgem by Sohn Associates Limited', 2006, Available from: https://www.ofgem.gov.uk/sites/default/files/docs/2009/05/sohn-overview-of-losses-final-internet-version.pdf

[4] Ma, K., Li, R., Li, F.: 'Quantification of additional asset reinforcement cost from 3-phase imbalance', *IEEE Trans. Power Syst.*, 2016, **31**, (4), pp. 2885–2891

[5] Siti, M.W., Nicolae, D.V., Jimoh, A.A., *et al.*: 'Reconfiguration and load balancing in the LV and MV distribution networks for optimal performance', *IEEE Trans. Power Deliv.*, 2007, **22**, (4), pp. 2534–2540

[6] Yan, S., Tan, S.C., Lee, C.K., *et al.*: 'Electric springs for reducing power imbalance in three-phase power systems', *IEEE Trans. Power Electron.*, 2015, **30**, (7), pp. 3601–3609

[7] Mokryani, G., Majumdar, A., Pal, B.C.: 'Probabilistic method for the operation of three-phase unbalanced active distribution networks', *IET Renew. Power Gener.*, 2016, **10**, (7), pp. 944–954

[8] Xu, T., Pan, J., Jiang, Y., *et al.*: 'The effect of three-phase voltage imbalance at PCC on solar panel output power'. *Procedia Comput. Sci.*, 2015, **52**, (1), pp. 1218–1224. Available from: http://dx.doi.org/10.1016/j.procs.2015.05.163

[9] Aramizu, J., Vieira, J.C.M.: 'Analysis of PV generation impacts on voltage imbalance and on voltage regulation in distribution networks'. IEEE Power and Energy Society General Meeting, Vancouver, BC, Canada, 2013, pp. 1–5

[10] Lico, P., Marinelli, M., Knezović, K., *et al.*: 'Phase balancing by means of electric vehicles single-phase connection shifting in a low voltage danish grid'. Proc. of the Universities Power Engineering Conf., Glasgow, UK, November 2015, vol. 2015, pp. 1–5

[11] Jin, P., Li, Y., Li, G., *et al.*: 'Optimized hierarchical power oscillations control for distributed generation under unbalanced conditions', *Appl. Energy*, 2017, **194**, pp. 343–352

[12] Singh, D., Misra, R.K., Mishra, S.: 'Distribution system feeder re-phasing considering voltage-dependency of loads', *Int. J. Electr. Power Energy Syst.*, 2016, **76**, pp. 107–119

[13] Kaveh, M.R., Hooshmand, R.A., Madani, S.M.: 'Simultaneous optimization of re-phasing, reconfiguration and dg placement in distribution networks using bf-sd algorithm', *Appl. Soft Comput.*, 2018, **62**, pp. 1044–1055

[14] Soltani, S., Rashidinejad, M., Abdollahi, A.: 'Stochastic multiobjective distribution systems phase balancing considering distributed energy resources', *IEEE Syst. J.*, 2017, **12**, (3), pp. 2866–2877

[15] Eftekhari, S., Sadegh, M.O.: 'The effect of load modelling on phase balancing in distribution networks using search harmony algorithm', *Int. J. Electr. Comput. Eng. (2088-8708)*, 2019, **9**, (3), pp. 1461–1471

[16] Borozan, V., Rajicic, D., Ackovski, R.: 'Minimum loss reconfiguration of unbalanced distribution networks', *IEEE Trans. Power Deliv.*, 1997, **12**, (1), pp. 435–442

[17] ABB: 'Working with the Trip Characteristic Curves of ABB SACE Low Voltage Circuit-Breakers', Technical Application Guide, 2001

[18] Cao, W., Wu, J., Jenkins, N., *et al.*: 'Operating principle of soft open points for electrical distribution network operation', *Appl. Energy*, 2016, **164**, pp. 245–257. Available from: http://dx.doi.org/10.1016/j.apenergy.2015.12.005

[19] Bloemink, J.M., Green, T.C.: 'Increasing distributed generation penetration using soft normally-open points'. IEEE PES General Meeting, PES 2010, Minneapolis, Minnesota, USA, 2010, pp. 1–8

[20] Bloemink, J.M., Green, T.C.: 'Increasing photovoltaic penetration with local energy storage and soft normally-open points'. IEEE Power and Energy Society General Meeting, Detroit, MI, USA, 2011, pp. 1–8

[21] Bloemink, J.M., Green, T.C.: 'Benefits of distribution-level power electronics for supporting distributed generation growth', *IEEE Trans. Power Deliv.*, 2013, **28**, (2), pp. 911–919

[22] Cao, W., Wu, J., Jenkins, N., *et al.*: 'Benefits analysis of soft open points for electrical distribution network operation', *Appl. Energy*, 2016, **165**, pp. 36–47. Available from: http://dx.doi.org/10.1016/j.apenergy.2015.12.022

[23] Cao, W., Wu, J., Jenkins, N.: 'Feeder load balancing in MV distribution networks using soft normally-open points'. IEEE PES Innovative Smart Grid Technologies Conf. Europe, 2015, Istanbul, Turkey, 2015-January, (January), pp. 1–6

[24] Bloemink, J.M., Green, T.C.: 'Required VSC efficiency for zero net-loss distribution network active compensation'. 2016 IEEE 7th Int. Symp. on Power Electronics for Distributed Generation Systems, PEDG 2016, Vancouver, BC, Canada, 2016

[25] Thomas, L.J., Burchill, A., Rogers, D.J., *et al.*: 'Assessing distribution network hosting capacity with the addition of soft open points', *IET Conf. Publications*, 2016, **2016**, (CP694), pp. 32 (6 .)–32 (6 .)

[26] Giannelos, S., Konstantelos, I., Strbac, G.: 'Stochastic optimisation-based valuation of smart grid options under firm DG contracts'. 2016 IEEE Int. Energy Conf., ENERGYCON 2016, Leuven, Belgium, 2016

[27] Konstantelos, I., Giannelos, S., Strbac, G.: 'Strategic valuation of smart grid technology options in distribution networks', *IEEE Trans. Power Syst.*, 2017, **32**, (2), pp. 1293–1303

[28] Bai, L., Jiang, T., Li, F., *et al.*: 'Distributed energy storage planning in soft open point based active distribution networks incorporating network reconfiguration and DG reactive power capability'. *Appl. Energy*, 2018, **210**, pp. 1082–1091. Available from: http://dx.doi.org/10.1016/j.apenergy.2017.07.004

[29] Wang, C., Song, G., Li, P., *et al.*: 'Optimal siting and sizing of soft open points in active electrical distribution networks', *Appl. Energy*, 2017, **189**, pp. 301–309. Available from: http://dx.doi.org/10.1016/j.apenergy.2016.12.075

[30] Qi, Q., Wu, J., Zhang, L., *et al.*: 'Multi-objective optimization of electrical distribution network operation considering reconfiguration and soft open points', *Energy Procedia*, 2016, **103**, (April), pp. 141–146

[31] Wang, C., Song, G., Li, P., *et al.*: 'Optimal configuration of soft open point for active distribution network based on mixed-integer second-order cone programming', *Energy Procedia*, 2016, **103**, (April), pp. 70–75. Available from: http://dx.doi.org/10.1016/j.egypro.2016.11.251

[32] Qi, Q., Wu, J.: 'Increasing distributed generation penetration using network reconfiguration and soft open points', *Energy Procedia*, 2017, **105**, pp. 2169–2174

[33] Ji, H., Wang, C., Li, P., *et al.*: 'An enhanced SOCP-based method for feeder load balancing using the multi-terminal soft open point in active distribution networks', *Appl. Energy*, 2017, **208**, (June), pp. 986–995. Available from: https://doi.org/10.1016/j.apenergy.2017.09.051

[34] Li, P., Ji, H., Wang, C., *et al.*: 'Optimal operation of soft open points in active distribution networks under three-phase unbalanced conditions', *IEEE Trans. Smart Grid*, 2019, **10**, (1), pp. 380–391

[35] Wang, Q., Liao, J., Su, Y., *et al.*: 'An optimal reactive power control method for distribution network with soft normally-open points and controlled air-conditioning loads', *Int. J. Electr. Power Energy Syst.*, 2018, **103**, (Dec. 2017.), pp. 421–430

[36] Ji, H., Wang, C., Li, P., *et al.*: 'Robust operation of soft open points in active distribution networks with high penetration of photovoltaic integration', *IEEE Trans. Sust. Energy*, 2019, **10**, (1), pp. 280–289

[37] Pereda, J., Green, T.C.: 'Direct modular multilevel converter with six branches for flexible distribution networks', *IEEE Trans. Power Deliv.*, 2016, **31**, (4), pp. 1728–1737

[38] Long, C., Wu, J., Thomas, L., *et al.*: 'Optimal operation of soft open points in medium voltage electrical distribution networks with distributed generation', *Appl. Energy*, 2016, **184**, pp. 427–437. Available from: http://dx.doi.org/10.1016/j.apenergy.2016.10.031

[39] Li, P., Ji, H., Wang, C., *et al.*: 'Coordinated control method of voltage and reactive power for active distribution networks based on soft open point', *IEEE Trans. Sust. Energy*, 2017, **8**, (4), pp. 1430–1442

[40] Ji, H., Yu, H., Song, G., *et al.*: 'A decentralized voltage control strategy of soft open points in active distribution networks', *Energy Procedia*, 2019, **159**, pp. 412–417

[41] Aithal, A., Long, C., Cao, W., *et al.*: 'Impact of soft open point on feeder automation'. 2016 IEEE Int. Energy Conf., ENERGYCON 2016, Leuven, Belgium, 2016

[42] Li, P., Song, G., Ji, H., *et al.*: 'A supply restoration method of distribution system based on soft open point'. IEEE PES Innovative Smart Grid Technologies Conf. Europe, Ljubljana, Slovenia, 2016

[43] Aithal, A., Li, G., Wu, J., *et al.*: 'Performance of an electrical distribution network with soft open point during a grid side AC fault', *Appl. Energy*, 2018, **227**, (August), pp. 262–272. Available from: http://dx.doi.org/10.1016/j.apenergy.2017.08.152

[44] Boyd, S., Vandenberghe, L.: '*Convex optimization*' (Cambridge University Press, Cambridge, England, UK, 2004)

[45] Sun, J., Tesfatsion, L.: 'DC Optimal Power Flow Formulation and Solution Using QuadProgJ', ISU Economics Working Paper No 06014, 2010, (March 1), pp. 1–62

[46] Coffrin, C., Van Hentenryck, P.: 'A linear-programming approximation of AC power flows', *INFORMS J. Comput.*, 2014, **26**, (4), pp. 718–734

[47] Castillo, A., Lipka, P., Watson, J.P., *et al.*: 'A successive linear programming approach to solving the IV-ACOPF', *IEEE Trans. Power Syst.*, 2016, **31**, (4), pp. 2752–2763

[48] Franco, J.F., Rider, M.J., Lavorato, M., *et al.*: 'A set of linear equations to calculate the steady-state operation of an electrical distribution system', 2011 IEEE PES Conf. on Innovative Smart Grid Technologies Latin America SGT LA 2011 - Conf. Proc., Medellin, Colombia, 2011

[49] Akbari, T., Bina, M.T.: 'Linear approximated formulation of AC optimal power flow using binary discretisation', *IET Gener. Trans. Distrib.*, 2016, **10**, (5), pp. 1117–1123

[50] Yuan, H., Li, F., Wei, Y., *et al.*: 'Novel linearized power flow and linearized OPF models for active distribution networks with application in distribution LMP', *IEEE Trans. Smart Grid*, 2018, **9**, (1), pp. 438–448

[51] Yang, Z., Zhong, H., Bose, A., *et al.*: 'A linearized OPF model with reactive power and voltage magnitude: a pathway to improve the MW-only DC OPF', *IEEE Trans. Power Syst.*, 2018, **33**, (2), pp. 1734–1745

[52] Jabr, R.A.: 'Exploiting sparsity in SDP relaxations of the OPF problem', *IEEE Trans. Power Syst.*, 2012, **27**, (2), pp. 1138–1139

[53] Wang, W., Yu, N.: 'Chordal conversion based convex iteration algorithm for three-phase optimal power flow problems', *IEEE Trans. Power Syst.*, 2018, **33**, (2), pp. 1603–1613

This is an open access article published by the IET under the Creative Commons Attribution License (http://creativecommons.org/licenses/by/3.0/)

[54] Dall'Anese, E., Zhu, H., Giannakis, G.B.: 'Distributed optimal power flow for smart microgrids', *IEEE Trans. Smart Grid*, 2013, **4**, (3), pp. 1464–1475
[55] Watson, J.D., Watson, N.R., Lestas, I.: 'Optimized dispatch of energy storage systems in unbalanced distribution networks', *IEEE Trans. Sust. Energy*, 2018, **9**, (2), pp. 639–650
[56] Araujo, L.R., Penido, D., Carneiro, S., *et al.*: 'A three-phase optimal power-flow algorithm to mitigate voltage unbalance', *IEEE Trans. Power Deliv.*, 2013, **28**, (4), pp. 2394–2402
[57] Araujo, L.R., Penido, D.R.R., de Alcântara-Vieira, F.: 'A multiphase optimal power flow algorithm for unbalanced distribution systems', *Int. J. Electr. Power Energy Syst.*, 2013, **53**, pp. 632–642
[58] Lee, C., Liu, C., Mehrotra, S., *et al.*: 'Robust distribution network reconfiguration', *IEEE Trans. Smart Grid*, 2015, **6**, (2), pp. 836–842
[59] Franco, J.F., Ochoa, L.F., Romero, R.: 'AC OPF for smart distribution networks: an efficient and robust quadratic approach', *IEEE Trans. Smart Grid*, 2018, **9**, (5), pp. 4613–4623
[60] Low, S.H.: 'Convex relaxation of optimal power flow - part i: formulations and equivalence', *IEEE Trans. Control Netw. Syst.*, 2014, **1**, (1), pp. 15–27
[61] Gan, L., Li, N., Topcu, U., *et al.*: 'Exact convex relaxation of optimal power flow in radial networks', *IEEE Trans. Autom. Control*, 2015, **60**, (1), pp. 72–87
[62] Nick, M., Cherkaoui, R., Boudec, J.Y.L., *et al.*: 'An exact convex formulation of the optimal power flow in radial distribution networks including transverse components', *IEEE Trans. Autom. Control*, 2018, **63**, (3), pp. 682–697
[63] Pillay, P., Manyage, M.: 'Definitions of voltage unbalance', *IEEE Power Eng. Rev.*, 2001, **21**, (5), pp. 50–51
[64] Funmilayo, H.B., Silva, J.A., Butler-Purry, K.L.: 'Overcurrent protection for the ieee 34-node radial test feeder', *IEEE Trans. Power Deliv.*, 2012, **27**, (2), pp. 459–468
[65] Schneider, K., Mather, B., Pal, B., *et al.*: 'Analytic considerations and design basis for the ieee distribution test feeders', *IEEE Trans. Power Syst.*, 2017, **33**, (3), pp. 3181–3188
[66] Kersting, W.H.: 'Radial distribution test feeders', *IEEE Trans. Power Syst.*, 1991, **6**, (3), pp. 975–985
[67] Kersting, W.H.: '*Distribution system modeling and analysis*' (CRC press, Boca Raton, FL, USA, 2006)
[68] Smith, A.: 'Electricity safety, quality and continuity regulations 2002', *Light. J.*, 2003, **68**, (2), pp. 35–36
[69] Bhutto, G.M., Bak-Jensen, B., Mahat, P., *et al.*: 'Mitigation of unbalanced voltage sags and voltage unbalance in cigre low voltage distribution network', *Energy Power Eng.*, 2013, **5**, (9), p. 551
[70] Lofberg, J.: 'Yalmip: a toolbox for modeling and optimization in matlab'. 2004 IEEE international conference on robotics and automation (IEEE Cat. No. 04CH37508). (IEEE), New Orleans, LA, USA, 2004, pp. 284–289
[71] Bixby, B.: 'The gurobi optimizer', *Transp. Re-search Part B*, 2007, **41**, (2), pp. 159–178, 2011
[72] Biegler, L.T., Zavala, V.M.: 'Large-scale nonlinear programming using ipopt: an integrating framework for enterprise-wide dynamic optimization', *Comput. Chem. Eng.*, 2009, **33**, (3), pp. 575–582

This is an open access article published by the IET under the Creative Commons Attribution License (http://creativecommons.org/licenses/by/3.0/)